FERMILAB-SLIDES-19-042-TD

Thermal contact resistance

R.C. Dhuley

CSA Short Course: Property and Cooler Considerations for Cryogenic Systems

Sunday, July 21 2019; CEC-ICMC 2019 at Hartford CT

Technical importance in cryogenics

Any cryogen-free system or a system seeking to be cryogen-free will encounter thermal contact resistance

- Sub-Kelvin experiments coupled to ADRs, dilution refrigerators, etc.
- Bath cooled systems seeking cryogen-independence *via* conductive coupling to cryocoolers

Undesired consequences of large thermal contact resistance:

- Long cooldown times
- Poor thermal equilibrium between experiment and cooler even when heats leaks are small
- Large sample-cooler temperature jump during operation (reduction in the range of operating temperatures)
- Each of the above issue will worsen with decreasing temperature!

Complexities:

- No unified or simple models: too many governing parameters
- Difficult experimental characterization

Outline and course objectives

Objectives: To understand the complexities of the problem, familiarize with existing theory to obtain rough estimates, learn how to characterize low temperature thermal contacts.

Outline:

- Origins and mechanisms
- Theoretical models for metallic contacts
  - 'macroscopic' constriction resistance
  - 'microscopic' boundary resistance
- Characteristics of contact resistance at low temperatures
- Measurement techniques
- Contact resistance R&D at Fermilab
  - SuperCDMS SNOLAB sub-Kelvin cryostat
  - Conduction cooling of an SRF niobium cavity
- Examples of data from the literature

Origins

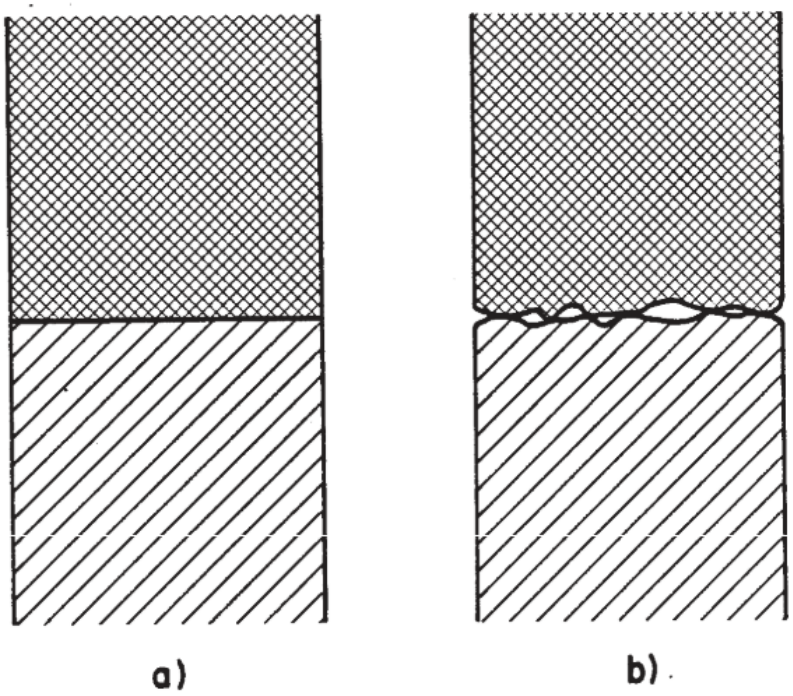

Ref: Van Sciver, Nellis, Pfotenhauer

Reduction in heat transfer area
- surface “waviness”, microscopic asperities (roughness)

Oxide surface layer (metals)

Surface films, adsorbed gases

Differential thermal contraction (cryogenic case)

The actual physical boundary (carrier reflection, scattering)

Contact heat transfer mechanisms

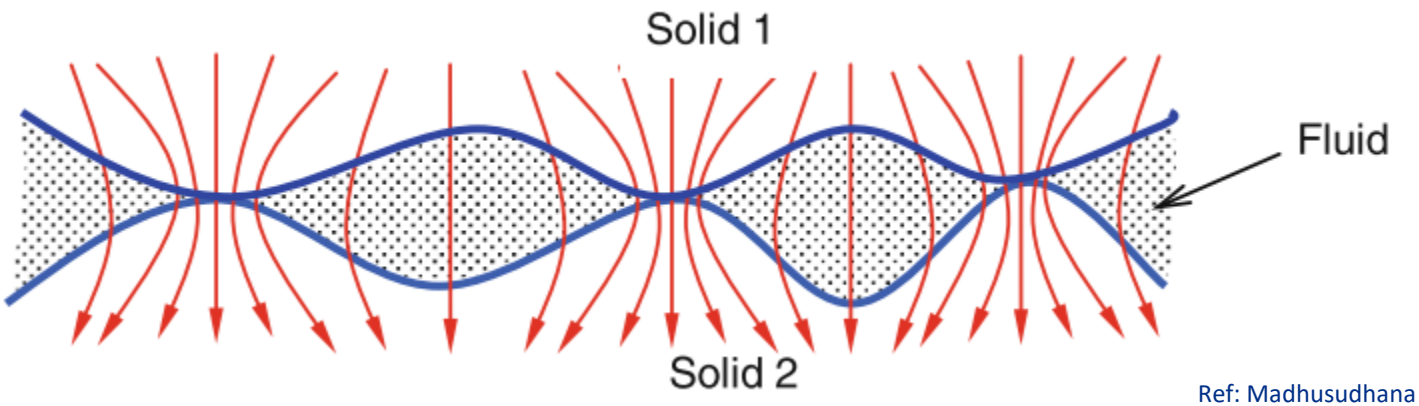

Ref: Madhusudhana

- Conduction through actual solid-solid contact spots (spot or constriction resistance)
  - **important for cryogenic applications**
- Conduction through interstitial medium, example air (gap resistance)
  - neglected if fluid is absent (eg. **vacuum in cryogenic systems**)
- Radiation
  - small unless T or ΔT are is large (**not significant at low T**)

Spot resistance, analyses

Heat flow analysis (thermal model)
- constriction resistance due to “thinning” of heat flow lines
- boundary reflection of heat carriers (electrons, phonons)
- determines the basic premise of contact resistance

Surface texture analysis (geometrical model)
- surface roughness, slope of as valleys and peaks
- determines number and size of contacting asperities

Asperity deformation analysis (mechanical model)
- Surface microhardness, elastic modulus, applied pressure/force
- determines the area of ‘real’ or physical contact
  (the surface area available for heat transfer)

Thermal analysis: macroscopic vs. microscopic

Differentiated based on spot "Knudsen" number

$$Kn = \frac{mean\ free\ path, l}{constriction\ size, a}$$

(equivalent of continuum and molecular flow regimes of gases)

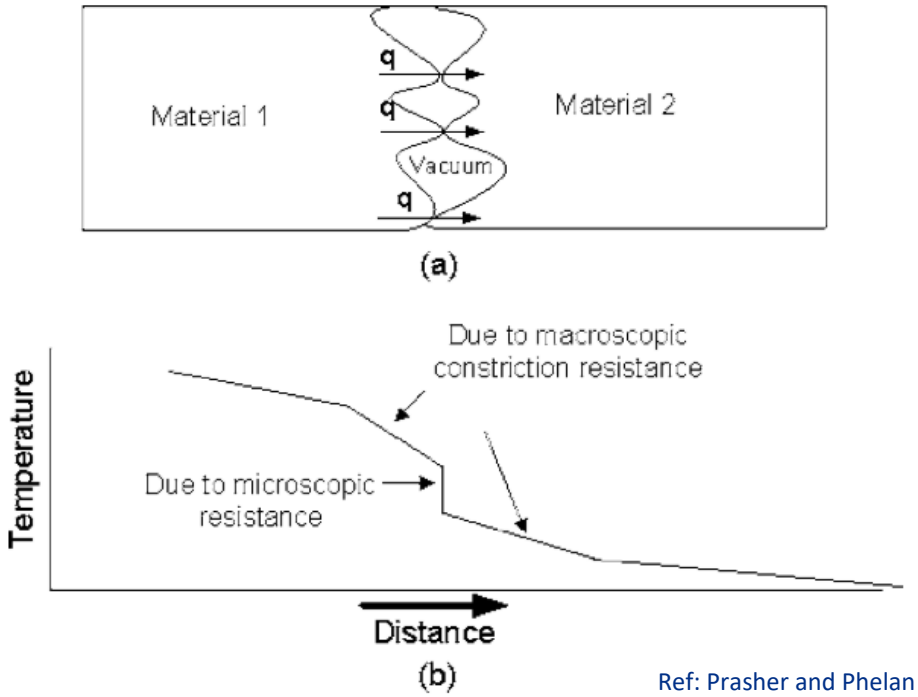

Ref: Prasher and Phelan

Major influencers

l: temperature and purity of metals (especially cryogenic conditions)

a: surface finish/roughness, machining processes

Fermilab

Thermal analysis: macroscopic vs. microscopic

Constriction resistance

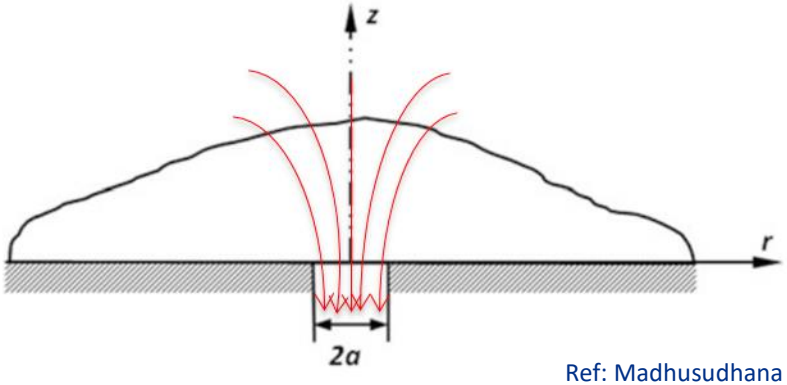

Ref: Madhusudhana

$$l << a$$

- diffusion limited thermal transport
- macroscopic component dominates

Boundary resistance

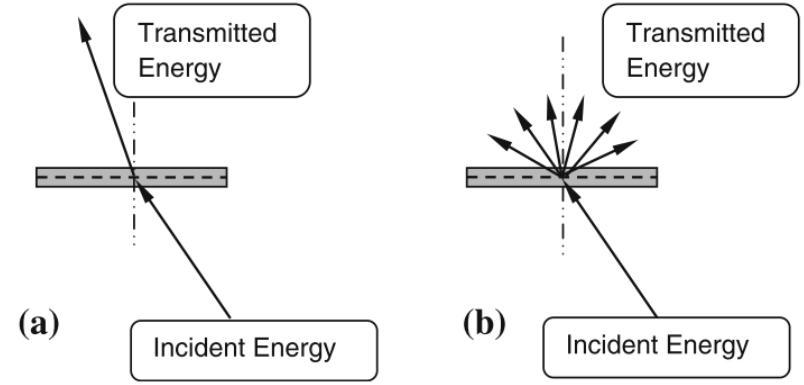

Ref: Madhusudhana

$$l >> a$$

- ballistic/boundary scattering effects
- microscopic component dominates

$$l \sim a$$: both effects important

Fermilab

Thermal analysis of a spot: macroscopic

- Macroscopic spot resistance ($l << a$): "bulk" thermal conductivity holds valid at the spot (diffusion regime)

Semi-infinite solid cylinder, with a round constriction

Ref: Madhusudhana

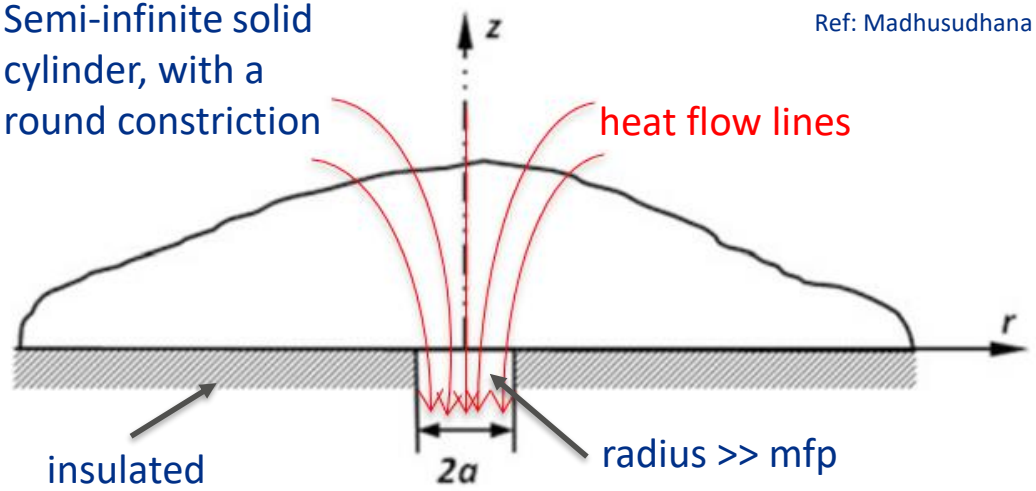

Analytical solution is obtained by solving the steady state heat diffusion in cylindrical coordinates

$$\frac{\partial^2 T}{\partial r^2} + \frac{1}{r}\frac{\partial T}{\partial r} + \frac{\partial^2 T}{\partial z^2} = 0$$

- Result (See textbook by C. V. Madhusudhana for analytical solution steps):

$$R_{macro,spot} = \frac{1}{4ak} = \frac{0.25}{ak}$$

Spot at uniform temperature

$$R_{macro,spot} = \frac{8}{3\pi a^2 k} = \frac{0.27}{ak}$$

Spot with uniform heat flux

- Unit is K/W
- Spot condition changes the solution by 8% (often negligible in practice)

Fermilab

Thermal analysis of spots in parallel, joints

- Bounded spot

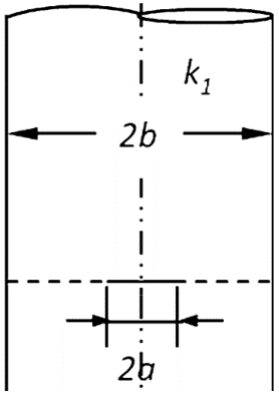

Ref: Madhusudhana

$$R_C = \frac{\psi(a/b)}{4ak}$$

- Ψ(a/b) is constriction alleviation factor (<1)
- Usable form is given later

- Bounded joint

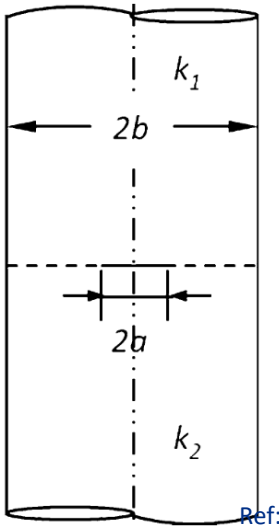

Ref: Madhusudhana

$$R_C = \frac{\psi(a/b)}{2ak_s}$$

$$k_s = \frac{2k_1k_2}{k_1 + k_2}$$

equivalent thermal conductivity

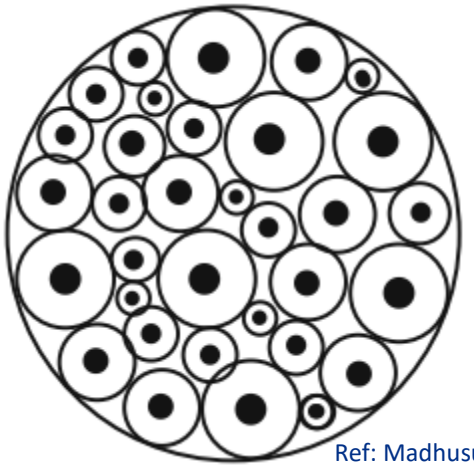
Ref: Madhusudhana

(idealized representation of contact plane)

- Contact with multiple spots

Parallel sum: $R_C^{-1} = \sum_i R_{Ci}^{-1}$

For *n* contacts of average size a_m and neglecting variation in Ψ :

$$R_C = \frac{\psi(a/b)}{2na_mk_s}$$

Surface topography (geometry) analysis

- The contacting surfaces are characterized in terms of their
  - Roughness (height distribution of peaks and valleys)
  - Asperity slope ('steepness' of peaks and valleys)

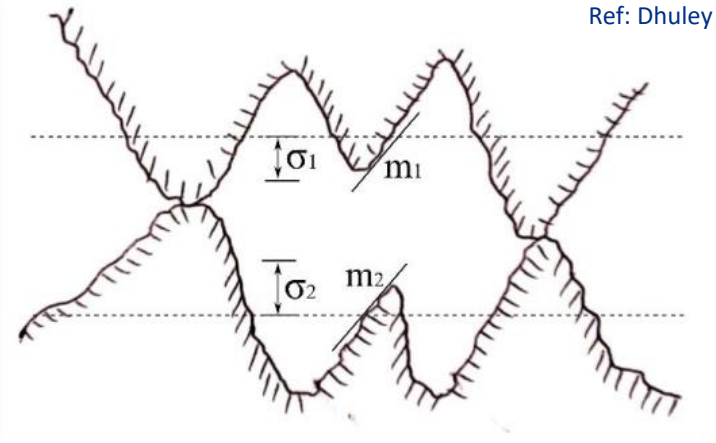

- These are essentially random, but are often assumed to have Gaussian distribution
  - σ = standard deviation of heights
  - m = standard deviation of slopes
- Relation to typically measured surface roughness

$$\sigma = R_q \approx \sqrt{\frac{\pi}{2}} R_a$$

where R_q is rms surface roughness

R_a is average surface roughness

Surface topography (geometry) analysis

- Determination of surface geometry parameters
  - Roughness parameter (z(x) is local height/depth)

$$R_a = \frac{1}{L_{sample}} \int_0^{L_{sample}} |z(x)|\,dx$$

measured using a profilometer (eq. laser scanning microscope)

  - Average asperity slope

$$m = \frac{1}{L_{sample}} \int_0^{L_{sample}} \left|\frac{dz(x)}{dx}\right| dx$$

computed from profilometer measurements

  - Empirical correlations (find m from known σ)

Table 1 Correlations for *m*, Gaussian surfaces

Reference	Correlation
Tanner and Fahoum [12]	$m=0.152\ \sigma^{0.4}$
Antonetti et al. [13]	$m=0.124\ \sigma^{0.743}$, $\sigma \leqslant 1.6\ \mu m$
Lambert and Fletcher [14]	$m=0.076\ \sigma^{0.52}$

Ref: Bahrami et al.

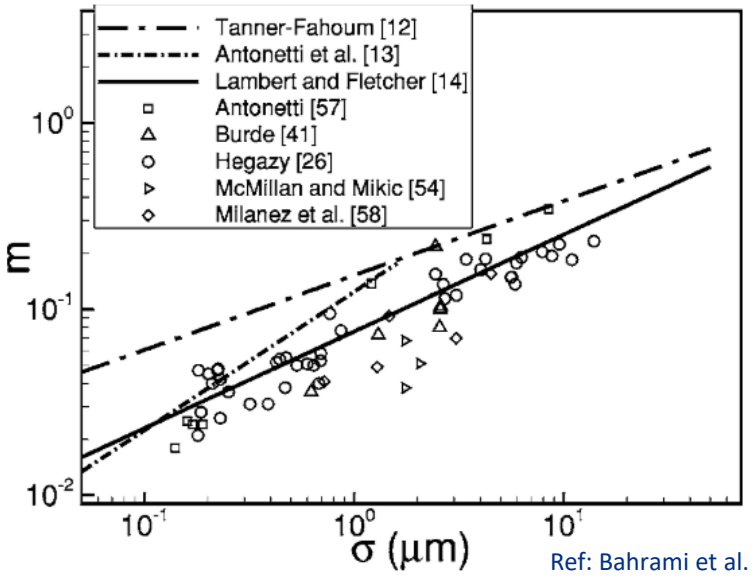

Ref: Bahrami et al.

Fermilab

Surface topography (geometry) analysis

- Equivalent roughness and surface slope are calculated as:

$$\sigma_s = \sqrt{\sigma_1^2 + \sigma_2^2}$$

$$m_s = \sqrt{m_1^2 + m_2^2}$$

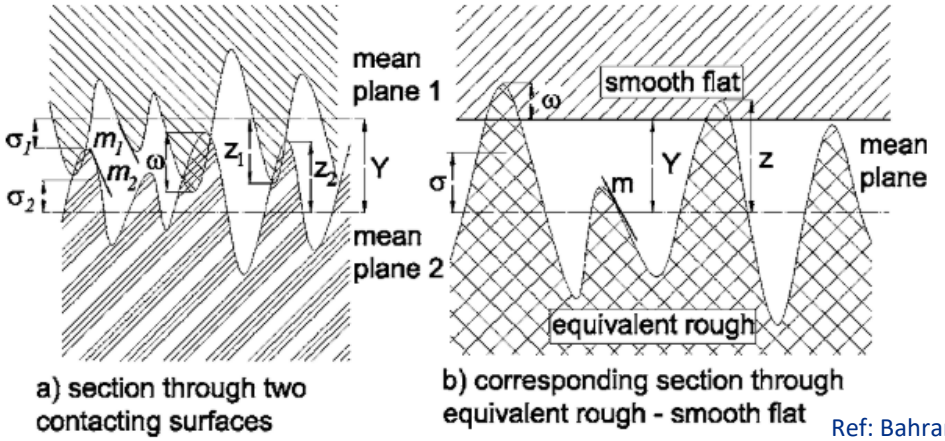

Ref: Bahrami et al.

- Average spot size (a_m) and number of spots per unit area (n) can be now be obtained as:

$$n\left(\pi a_m^2\right) = \frac{A_{real}}{A_{apparent}} \qquad a_m = 4\left(\frac{\sigma_s}{m_s}\right)\left(\frac{A_{real}}{A_{apparant}}\right)\exp\left[\left\{erfc^{-1}\left(\frac{2A_{real}}{A_{apparent}}\right)\right\}^2\right]$$ for circular contacts

Note: $A_{real}/A_{apparent}$ is still unknown and is obtained via deformation analysis

Fermilab

Asperity deformation analysis

- Asperities deform ‘heavily’ because the tiny contact area they represent supports all the applied load

- Deformation, whether elastic or plastic, can be determined by evaluating a plasticity index (several have been proposed)

  - Greenwood index: $\psi_G = \left(\frac{E'}{H_{micro}} \right) m_s$

    where $E' = 2\left(\frac{1-\nu_1^2}{E_1} - \frac{1-\nu_2^2}{E_2} \right)^{-1}$ is effective elastic modulus in terms of the individual elastic modulus and Poisson’s ratio; and H is microhardness of the softer material.

  - Plastic contacts: $\psi_G > 1$ - freshly prepared rough surfaces
  - Elastic contacts: $\psi_G < 0.7$ - polished surfaces; subsequent contact of plastically deformed surfaces

Asperity deformation analysis

- For a plastically deformed contact, the ratio of real contact area to apparent contact area is given by:

$$\frac{A_{real}}{A_{apparent}} = \frac{P_{applied}}{H_{micro}}$$ holds for $10^{-4} < \frac{P_{applied}}{H_{micro}} < 10^{-2}$ and a constant value of H_{micro}

$$\frac{A_{real}}{A_{apparent}} = \frac{P_{applied}}{H_{micro} + P_{applied}}$$ for larger loads

- H_{micro} is Vickers microhardness; can be approximated as 3*yield strength if microhardness is not readily available.
- Microhardness is indentation depth dependent and therefore a function of the surface roughness (asperity heights)

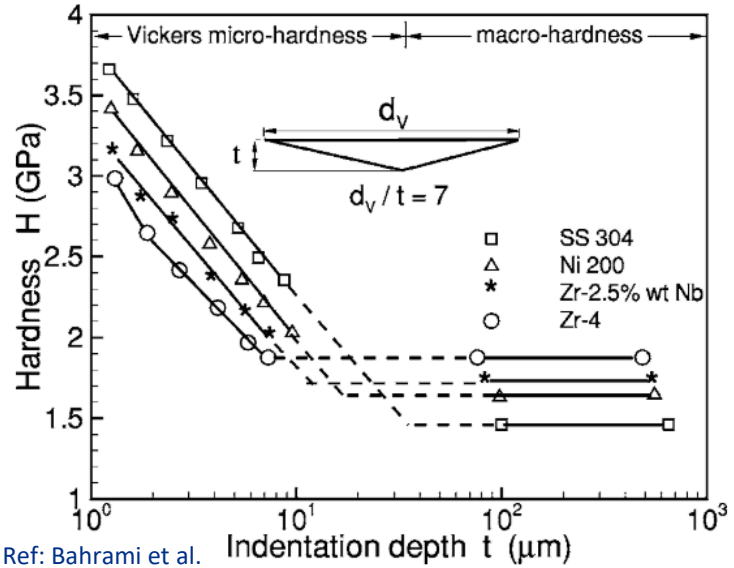

Ref: Bahrami et al.

Fermilab

Asperity deformation analysis

- For an elastically deformed contact, the ratio of real contact area to apparent contact area is given by:

$$\frac{A_{real}}{A_{apparent}} = \frac{1.41 P_{applied}}{E' m_s}$$

asperities are spherically shaped and have Gaussian distribution of heights

- **Note**: For both plastic and elastic contacts,

$$A_{real} \propto P_{applied} * A_{apparent} = F_{applied}$$

that is, the applied force determines the real contact area. Since contact resistance ~ real area, it is the applied force that dictates the determines. If the force is unchanged, contact resistance would not change with size of the contact.

Asperity deformation analysis

- Now that we have the ratio $A_{real}/A_{apparent}$, average spot size and spots per unit area can be approximated.
- The constriction factor $\Psi(a/b)$ from the thermal model can also be expressed in terms of the area ratio.
- Researchers have derived several expressions for these. Given below are expressions derived by Antonetti and Yovanovich:

$$a_m = 0.77\left(\frac{\sigma_s}{m_s}\right)\left(\frac{p_{applied}}{H_{micro}}\right)^{0.097} \qquad n\left(\pi a_m^2\right) = \frac{A_{real}}{A_{apparent}} \qquad \psi = 0.76\left(\frac{p_{applied}}{H_{micro}}\right)^{-0.027}$$

- The knowledge of n, a_m, and Ψ yields the macroscopic spot resistance.
- There are several models for the macroscopic contact resistance depending upon the model used for a_m, n, and F.

Macroscopic contact thermal resistance

- For flat, conforming contacts with **plastic** deformation, the expression for contact resistance has the form:

$$R_C = \frac{1}{A}\left(\frac{\sigma_s}{m_s}\right)\frac{1}{k_s}\left(\frac{p_{applied}}{H_{micro}}\right)^{-B}$$

K*m^2/W, expressed in terms of the apparent contact area;
usable for $10^{-4} < p_{applied}/H_{micro} < 10^{-2}$

Model	A	B
Cooper, Mikic, Yovanovich	1.45	0.985
Yovanovich	1.25	0.95
Tien	0.55	0.85
Wheeler	1.13	0.94
Mikic and Rohsenow	0.9	0.941

- See review paper by Lambert and Fletcher for more models, range of validity, etc. (https://arc.aiaa.org/doi/10.2514/2.6221)

Macroscopic contact thermal resistance

- For flat, conforming contacts with **elastic** deformation, the expression for contact resistance has the form:

$$R_C = \frac{1}{A}\left(\frac{\sigma_s}{m_s}\right)\frac{1}{k_s}\left(\frac{\sqrt{2}\,p_{applied}}{E' m_s}\right)^{-B}$$

K*m^2/W, expressed in terms of the apparent contact area

Model	A	B
Mikic	1.55	0.94
Greenwood and Williamson	1.75-1.87	0.95
Onions and Archard	2.38-2.8	0.97
Bush, Gibson, and Thomas	0.799	0.98

- See review paper by Lambert and Fletcher for more models, range of validity, etc. (https://arc.aiaa.org/doi/10.2514/2.6221)

Thermal analysis: microscopic

- Microscopic spot resistivity ($l >> a$): “bulk” thermal conductivity does not hold validity at the spot (Knudsen regime).
- Heat carriers (free electrons, phonons) on incidence with the physical boundary can reflect back or transmit on to the other side.

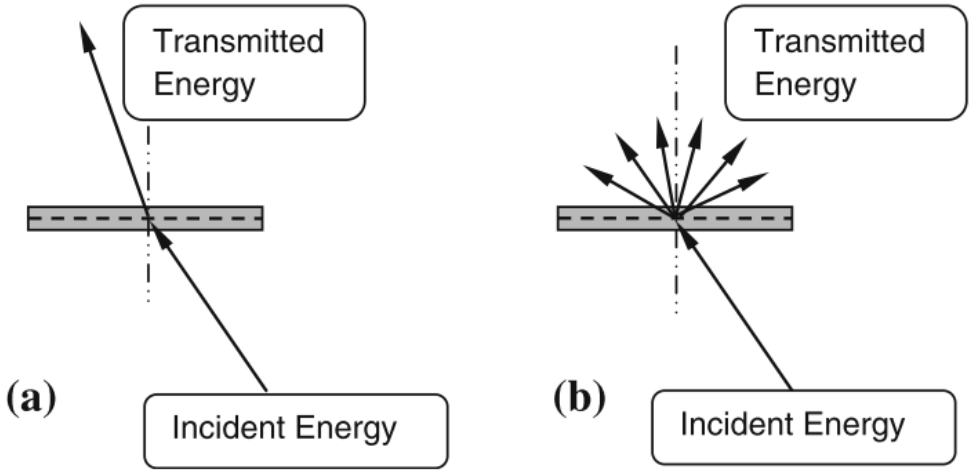

Ref: Madhusudhana

- Analytical solution is obtained by solving the fundamental energy transport equation (Landauer formalism) by assuming a proper transmission probability of the heat carriers.

Thermal analysis: microscopic

- Fundamental heat transport equation (see Swartz and Pohl's review 1988)
  - Electronic transport (metal-metal interfaces) from side '1' to '2'

$$q_{1\to 2,net} = \frac{1}{2}\int_0^{\pi/2}\int_0^{\infty} v_1[N_1(E,T_1) - N_1(E,T_2)]\alpha_{1\to 2}(E,\theta)\cos\theta\sin\theta d\theta E dE$$

Speed — Number density — Transmission probability — Energy

  - Phonon transport (metal-dielectric, metal-superconductor interfaces at low temperatures) from side '1' to '2'

$$q_{1\to 2,net} = \frac{1}{2}\sum_j \int_0^{\pi/2}\int_0^{\omega_{\max}} c_{1,j}[N_1(\omega,T_1) - N_1(\omega,T_2)]\alpha_{1\to 2}(\omega,\theta,j)\cos\theta\sin\theta d\theta \hbar\omega d\omega$$

Sum over three polarizations — Energy

- Figuring out the transmission probability is the main challenge!

Thermal analysis: microscopic

- Acoustic mismatch model for phonon transmission probability
  - Assumes a 'perfect' interface and specular transmission (Little, 1959)
  - The transmission is limited by acoustic impedance mismatch of the two sides
  - Works generally at extremely low temperatures (<1 K) where phonon wavelength is much larger than interface disorder

$$R_B(T) = \left[\frac{\pi^2}{15} \frac{k_B^2}{\hbar^3} \sum_j c_{1,j}^{-2} \Gamma_{1,j} \right]^{-1} T^{-3}$$

c_1 = phonon (sound) speed on side 1
j = phonon polarization (longitudinal, transverse)
Γ = transmission probability factor (requires numerical calculation, see paper by Cheeke, Ettinger, Hebral)

- Diffuse mismatch model for phonon transmission probability
  - All phonon incident on the interface scatter diffusively, forward scattering probability equals ratio of density of phonon states (Swartz and Polh, 1989)
  - Works at warmer temperatures where phonon wavelength is comparable to interface disorder

$$R_B(T) = \left[\frac{\pi^2}{15} \frac{k_B^2}{\hbar^3} \frac{1}{2} \frac{\sum_j c_{1,j}^{-2} \sum_j c_{2,j}^{-2}}{\sum_{i,j} c_{i,j}^{-2}} \right]^{-1} T^{-3}$$

Expression valid at temperature << Debye temperature

Thermal analysis: microscopic

- Diffuse mismatch model for electron transmission probability
  - All electrons incident on the interface scatter diffusively, forward scattering probability equals ratio of density of electron states (Gundrum *et al.*, 2005)
  - Analogy drawn from phonon diffuse mismatch model, not has been verified as extensively!

$$R_B(T) = \frac{6}{k_B^2}\frac{\hbar}{m_e}\left(\frac{E_{F1}}{v_{F1}^4} + \frac{E_{F2}}{v_{F2}^4}\right)T^{-1}$$

Expression valid at temperature << Fermi temperature; E_F, v_F are Fermi energy and Fermi velocity; n_e is free electron density (see book by Charles Kittel)

- Notes
  - Phonon models predict T^{-3} dependence, as is seen often times for metal-dielectric and metal-superconductor contacts at low temperatures (<< Debye temperature).
  - Electron model predicts T^{-1} dependence, as is common with well prepared clean metal-metal contacts (eg. gold plated copper). Gundrum *et al.* saw T^{-1} for Cu-Al contacts even in 77 – 300 K.
  - These model need $A_{real}/A_{apparent}$ ratio for use with pressed contacts

A simple model for pressed contacts

- The contacts are assumed to be flat and conforming

- Metal-metal contacts

$$R_B(T) = \frac{1}{A}\left(\frac{\sigma_s}{m_s}\right)\frac{1}{k_s}\left(\frac{p_{applied}}{H_{micro}}\right)^{-B} + \frac{6}{k_B^2}\frac{\hbar}{m_e}\left(\frac{E_{F1}}{v_{F1}^4} + \frac{E_{F2}}{v_{F2}^4}\right)T^{-1}\left(\frac{p_{applied}}{H_{micro}}\right)^{-1}$$

$= (A_{real}/A_{apparent})^{-1}$

- Metal-dielectric, metal-superconductor contacts

$$R_B(T) = \frac{1}{A}\left(\frac{\sigma_s}{m_s}\right)\frac{1}{k_s}\left(\frac{p_{applied}}{H_{micro}}\right)^{-B} + \left[\frac{\pi^2}{15}\frac{k_B^2}{\hbar^3}\frac{1}{2}\frac{\sum_j c_{1,j}^{-2}\sum_j c_{2,j}^{-2}}{\sum_{i,j} c_{i,j}^{-2}}\right]^{-1} T^{-3}\left(\frac{p_{applied}}{H_{micro}}\right)^{-1}$$

Common observations at low temperature (LHe)

- Dependence on temperature

  $R_C \sim T^{-1}$: pure or lightly oxidized metallic contacts (oxide<<deBroglie $\lambda_{electron}$)

  $R_C \sim T^{-2}$: oxidized metallic contacts (deBroglie $\lambda_{electron}$<<oxide<<λ_{phonon})

  $R_C \sim T^{-2<n<-1}$: practical metallic contacts (limited exposure to oxygen)

  $R_C \sim T^{-3}$: contact with a superconductor (T<<T_{crit})

- Weideman Franz law analogy for contacts

$$R_{C,thermal} = \frac{R_{C,elec}}{L_0} T^{-1}$$

L_0 is theoretical Lorenz number (=2.44x10^{-8} WΩ/K^2)

  - $R_{C,thermal} \sim T^{-1}$ at lower temperature since $R_{C,elec}$ is constant
  - Gives an upper bound of thermal contact resistance as an additional heat transfer channel (phonon) can be present.

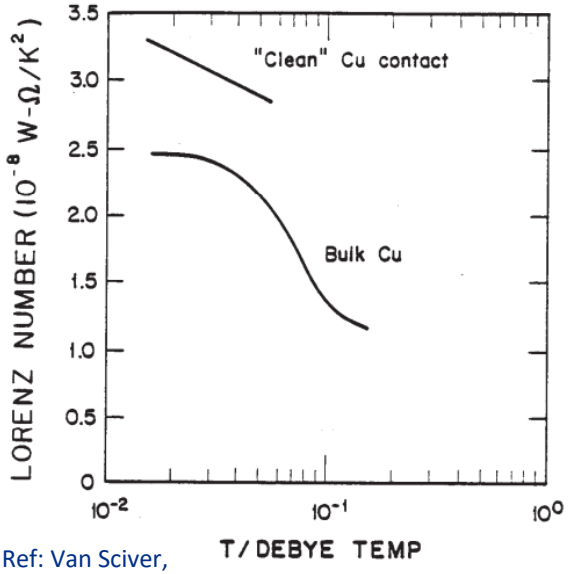

Ref: Van Sciver, Nellis, Pfotenhauer

Fermilab

Measurement techniques

- Steady state heat flow method
  - Uses a heater (*H*) to set up a heat flow across the contact and two thermometers (T_1, T_2) to measure temperature jump

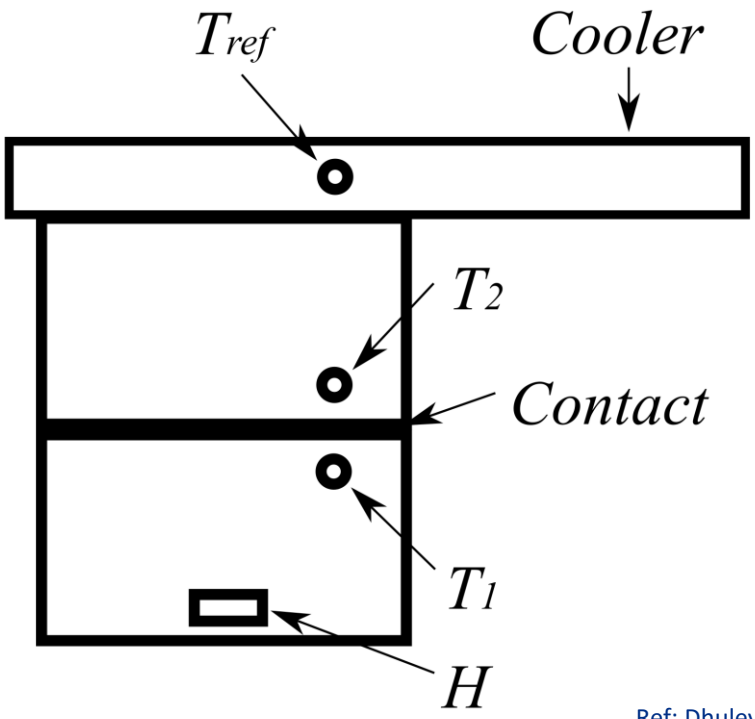

Ref: Dhuley

Steady state heat flow method implemented on a cryocooler

Contact resistance is determined as:

$$R_C(T_{avg}) = \frac{T_1 - T_2}{H} \quad \text{with} \quad T_{avg} = 0.5(T_1 + T_2)$$

Notes:

- Keep $T_1 - T_2$ < 1-2 % of T_{avg} to accurately capture the power law
- Locate thermometers as close to the contact as practical
- Systematic uncertainty in $T_1 - T_2$ can be significant, especially for small $T_1 - T_2$

Measurement techniques

- Two-heater method
  - Uses a thermometer (T) upstream and two heaters (H_1, H_2) across the contact
  - Two-step measurement: (a) $H_1 = H$, $H_2 = 0$, note $T = T_a$
    (b) $H_1 = 0$, $H_2 = H$, note $T = T_b$

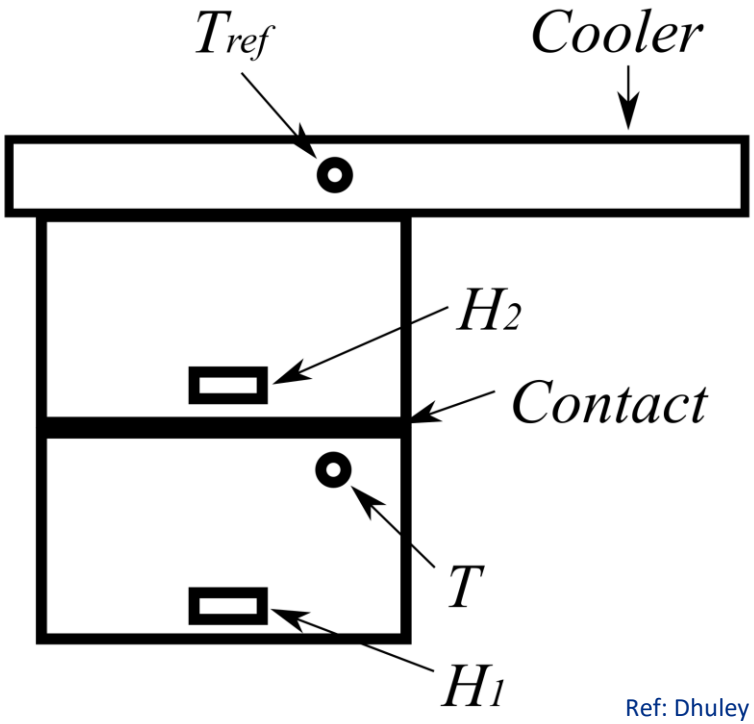

Ref: Dhuley

Two-heater method implemented on a cryocooler

Contact resistance is determined as:

$$R_C(T_{avg}) = \frac{T_a - T_b}{H} \quad \text{with } T_{avg} = 0.5(T_a + T_b)$$

Notes:

- To work, the method needs H to be "equal" in steps a and b => careful evaluation of heater wire heat leak
- Systematic uncertainty in $T_1 - T_2$ can be very small, especially for small $T_1 - T_2$

Measurement techniques

- Electrical contact resistance
  - Useful for metal-metal contacts near and below liquid helium temperature where the Wiedeman Franz law holds
  - In practice, measurements are done at 4.2 K to determine upper bound of thermal contact resistance; extrapolate to lower temperature using WF law
  - Measurement is much easier (and faster) that direct thermal resistance

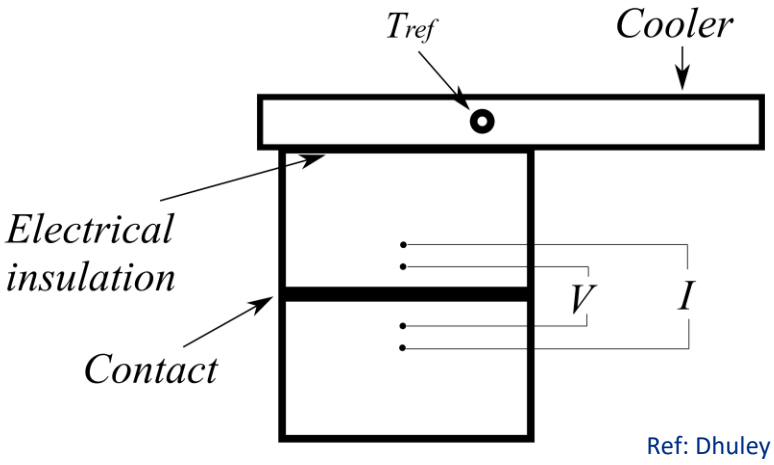

Ref: Dhuley

DC 4-wire measurement can yield few tenths of a μΩ

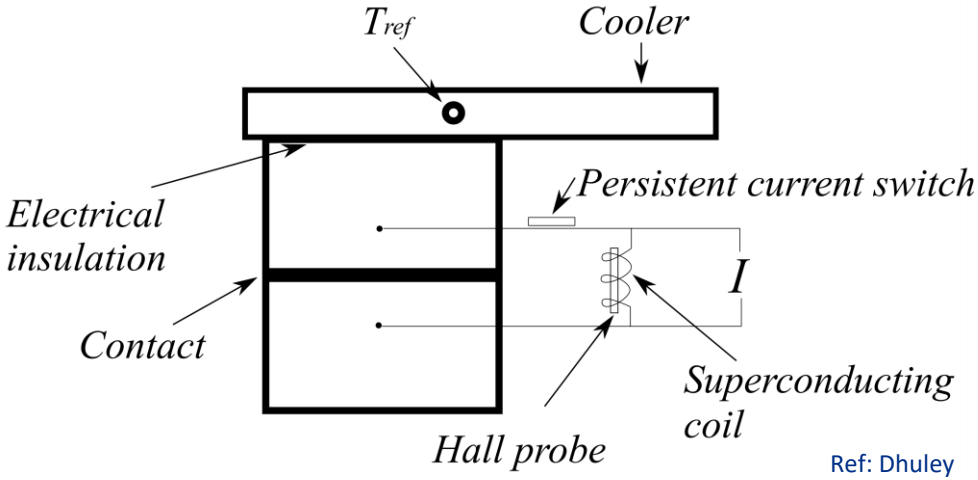

Ref: Dhuley

Current decay technique is found to be suitable to measure as low as a few nΩ

Example: SuperCDMS SNOLAB cryostat

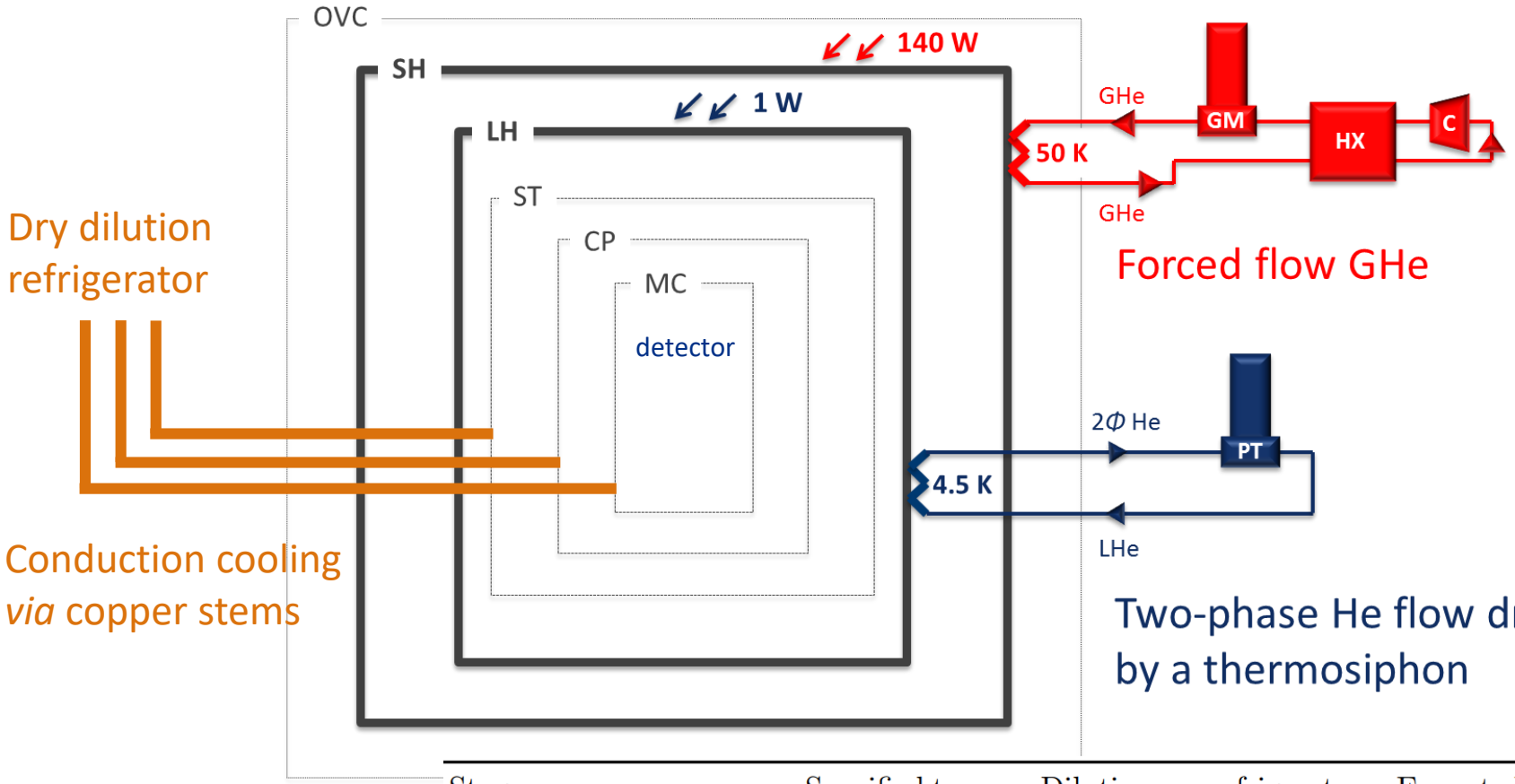

Sub-Kelvin requirements

Stage	Specified tower temperature	Dilution refrigerator cooling budget	Expected heat load
Mixing chamber (MC)	15 mK	5 μW @ 10 mK	1.6 μW
Cold plate (CP)	250 mK	350 μW @ 230 mK	115 μW
Still (ST)	1 K	15 mW @ 800 mK	4.1 mW

Example: SuperCDMS SNOLAB cryostat

Sub-Kelvin conduction stems (8 feet long): contacts (flat, cylindrical), flex straps

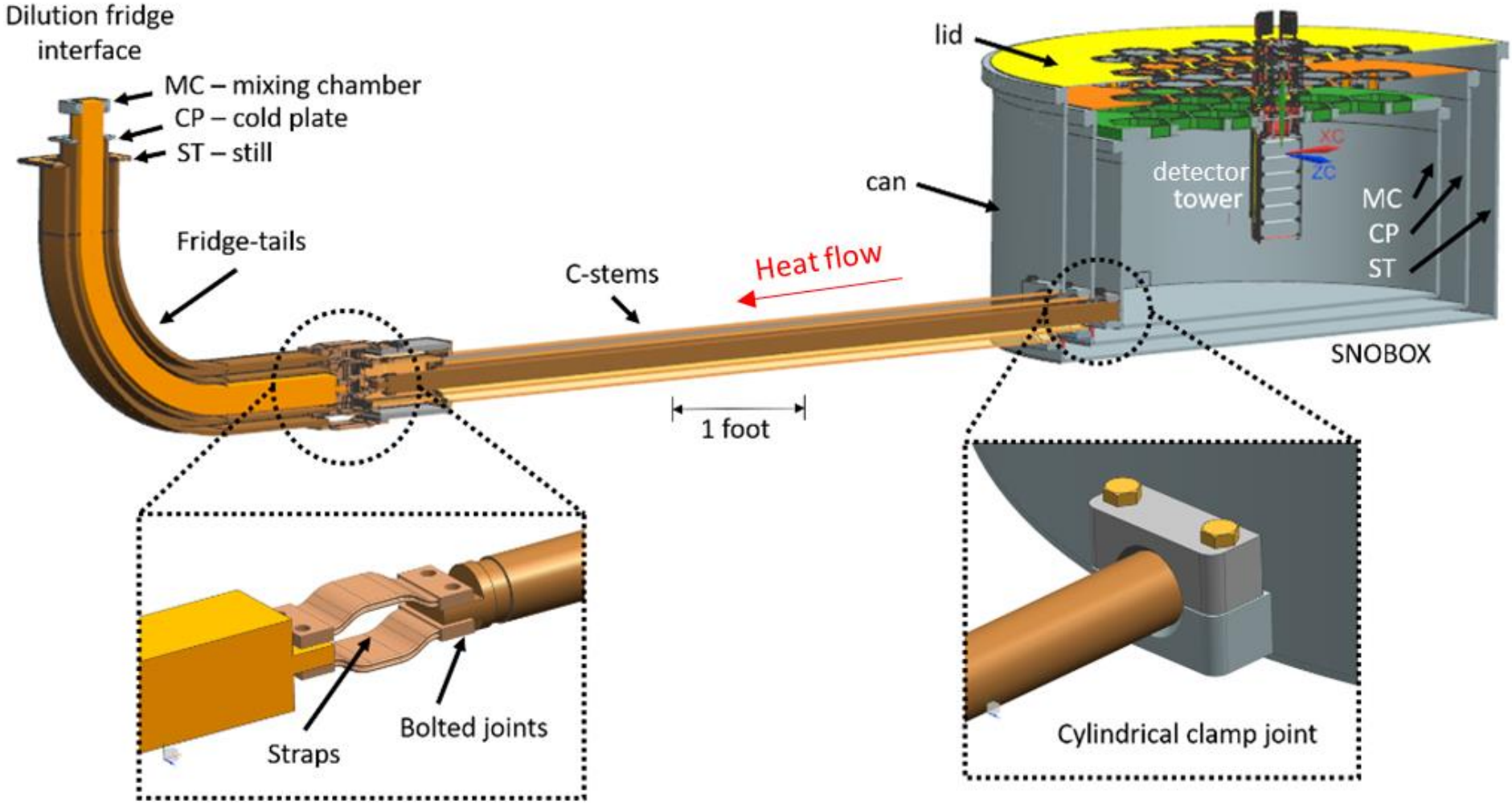

Dhuley et al.: https://doi.org/10.1088/1757-899X/278/1/012157

Fermilab

Conduction stem: Flat and cylindrical joints

Copper-copper joints

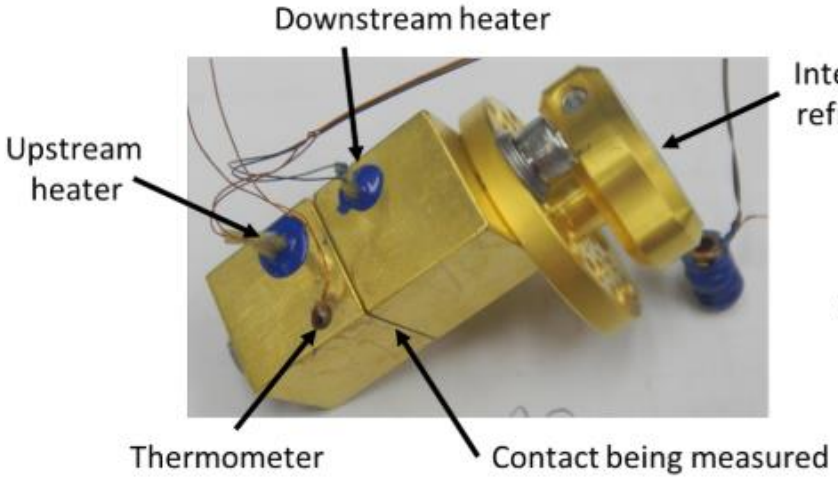

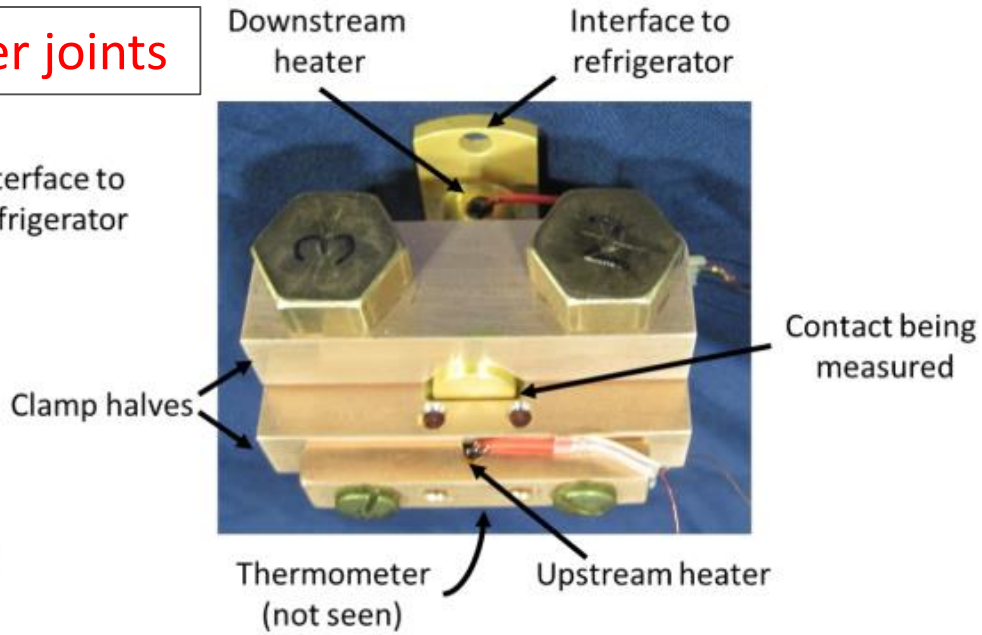

- Surface roughness = 0.2 µm
- Gold plating 0.5 µm over a nickel plate of 1.2 µm (better adhesion)
- Pressed using Belleville disc washers or differential thermal contraction between screw (brass) and plates (copper): Force ~3 kN
- Measured between 60 mK and 10 K (dilution fridge, ADR, pulse tube)

Conduction stem: Flexible linkages

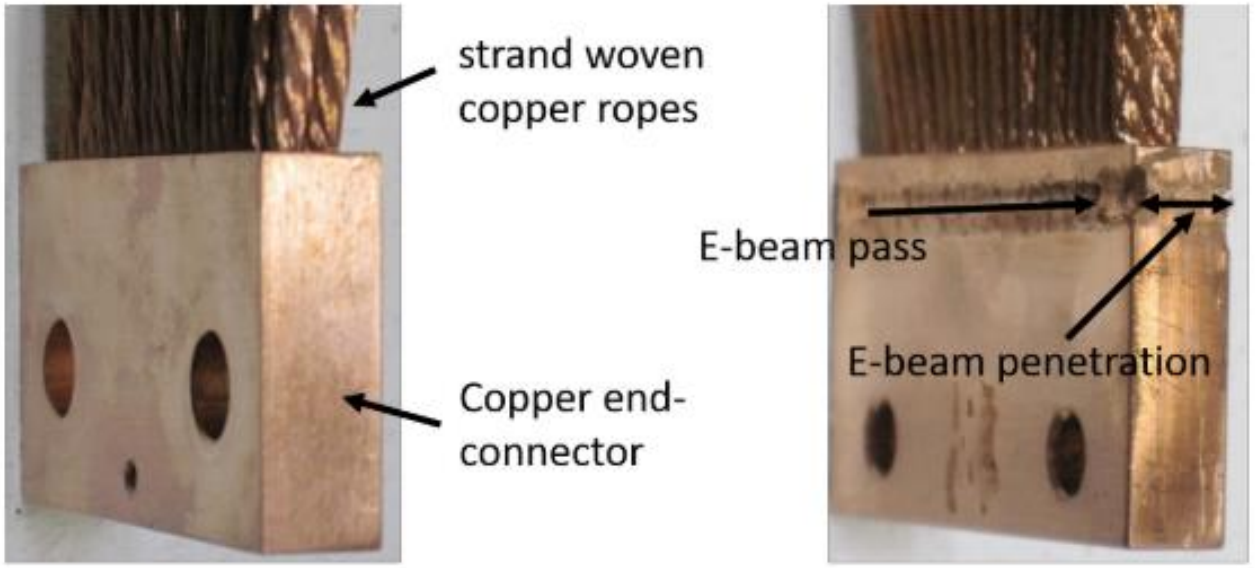

Commercial off-the-shelf thermal strap

- Works well above 1 K - controlled by conductance of flex ropes
- Not suitable <1 K – contact resistance at the end-connectors starts to dominate
- E-beam welding fused the ropes to the end-connector, made the strap suitable for <1 K use

Contact resistance measurements for SuperCDMS

Sub-Kelvin measurements on an ADR using the two-heater method

Flat joint

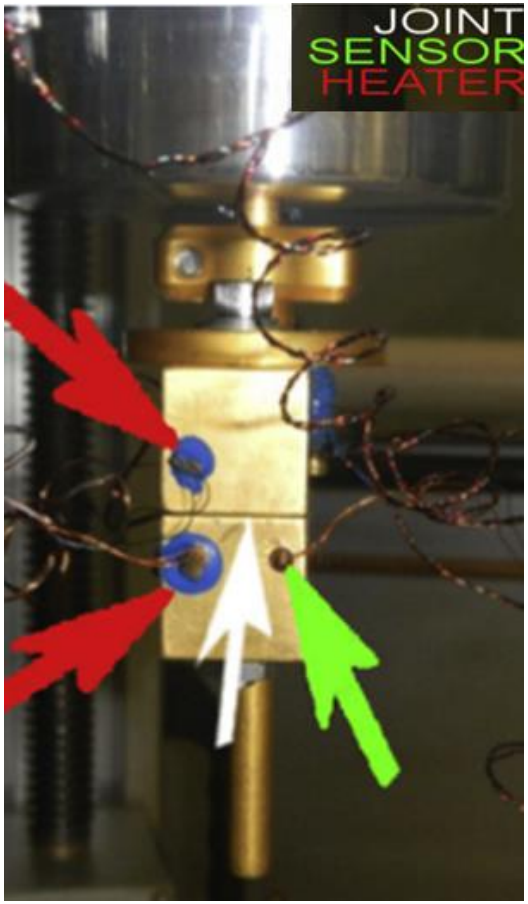

Cylindrical joint

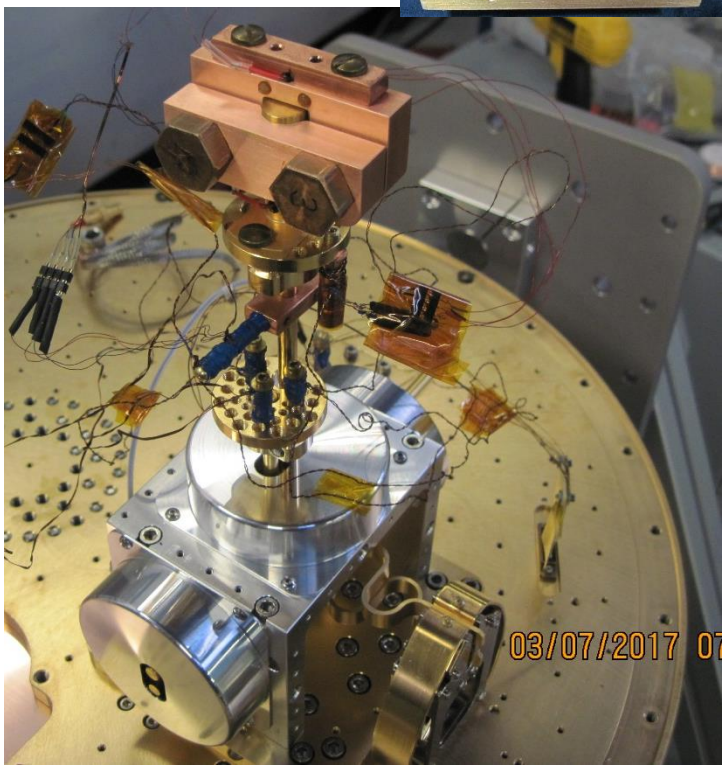

Flex strap

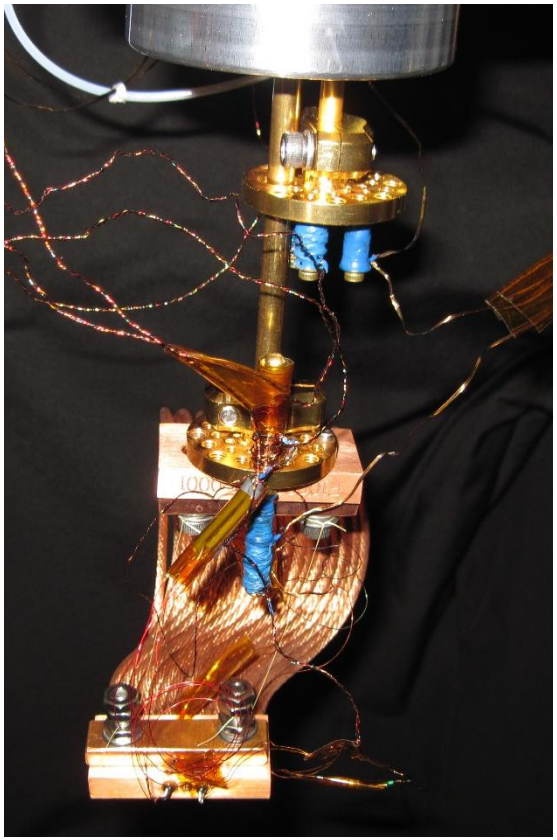

Fermilab

Results: conductance vs. temperature

Flat and cylindrical contacts

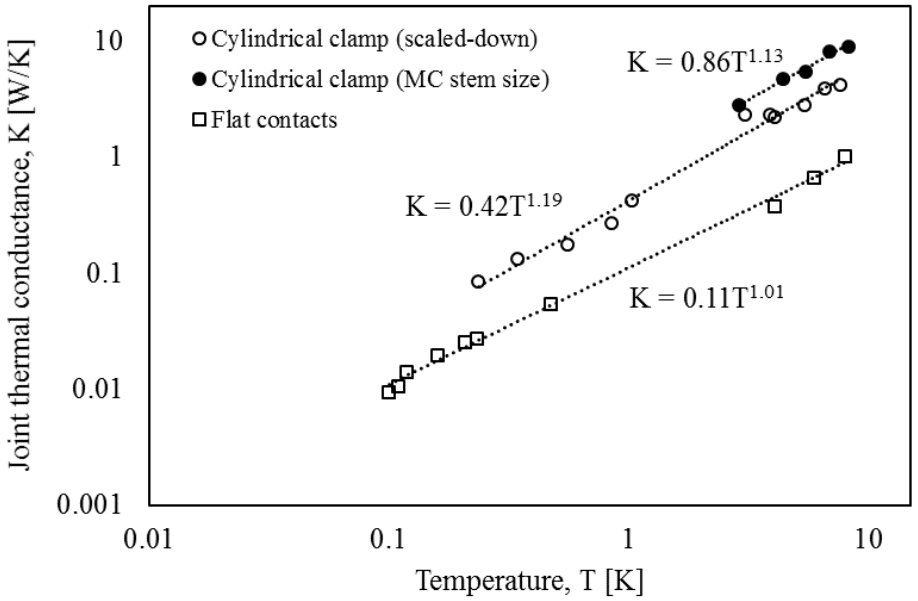

Flex straps

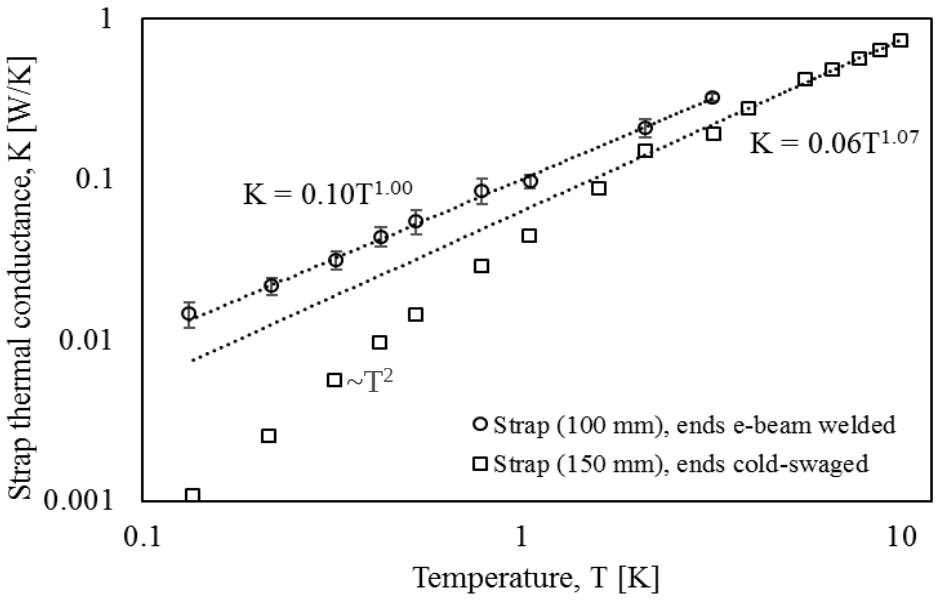

- Gold plated contacts produced nearly ~T^1 conductance

- Pressed straps yielded ~T^2 below 1 K (ropes/end connector may have carried copper oxide during swaging)
- Welding fused the ropes with end-connector, and produced ~T^1

Example: Conduction cooled SRF cavity

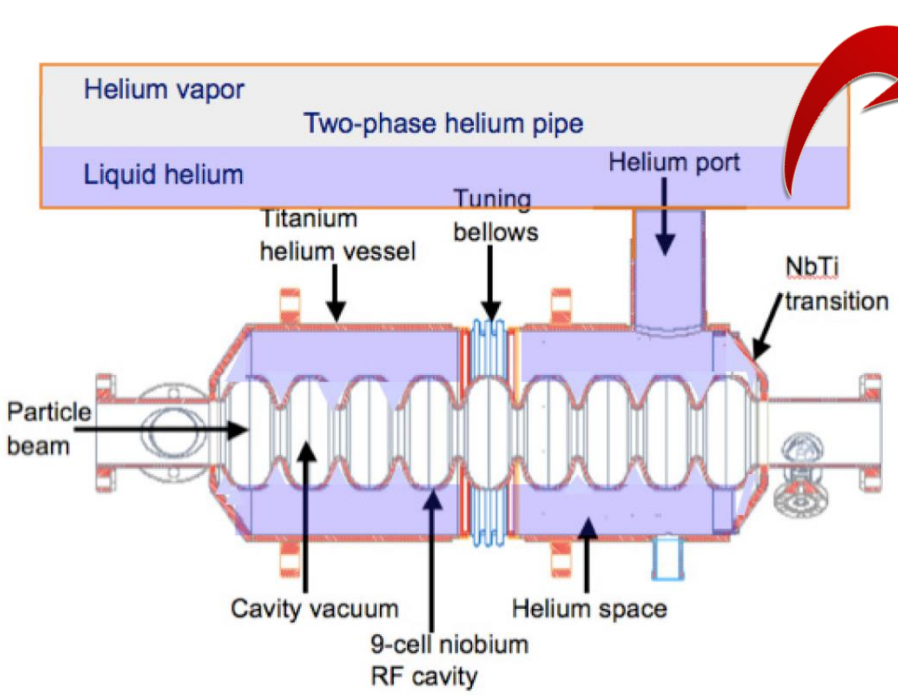

Take out liquid helium
(and its complexities)

Conduction-cool with
a cryocooler

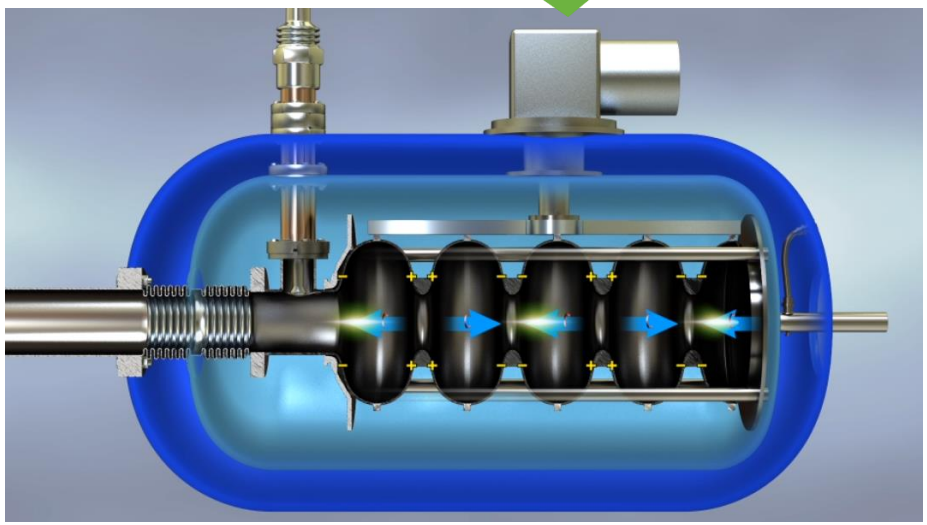

Fermilab

Example: Conduction cooled SRF cavity

Niobium SRF cavity dissipates heat when exposed to RF fields

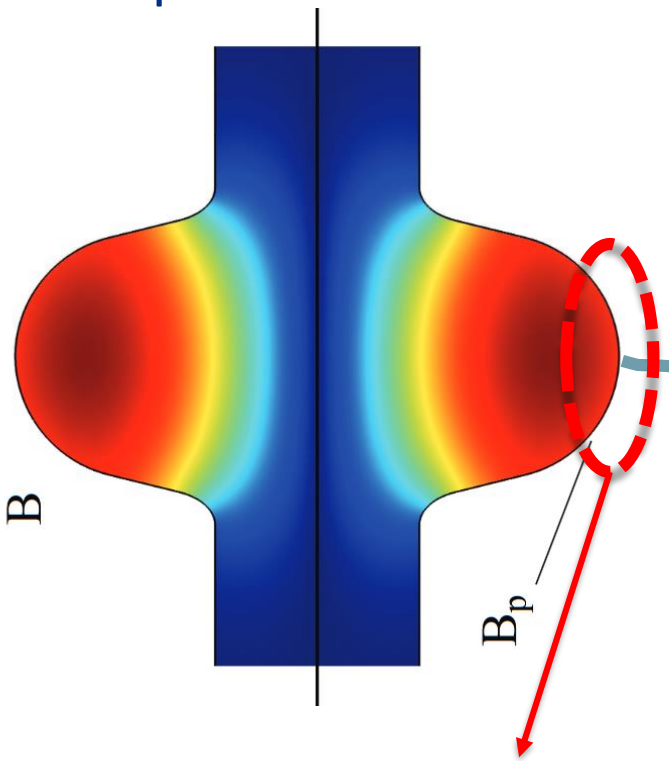

High conductance "metallic" link

Metal-superconductor pressed thermal contact!

Courtesy: Cryomech, Inc.

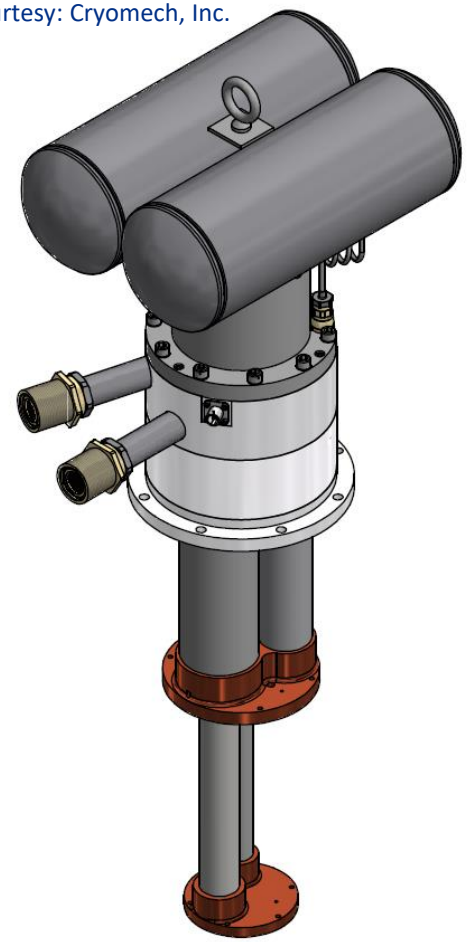

Pulse tube cryocooler absorbs the heat

Metal-superconductor joints for conduction cooling

Joint material:

5N aluminum (Al), SRF grade niobium (Nb)

Surface prep:

Roughness ≈ 1 μm

Cleaning: Al plate in NaOH solution

Nb plate *via* BCP

Force application:

Belleville disc washers of various stiffnesses (also help maintain bolt tension); range 4 – 14 kN

Contact resistance measurements:

T = 3 – 5 K, two-heater method, pulse tube cryocooler

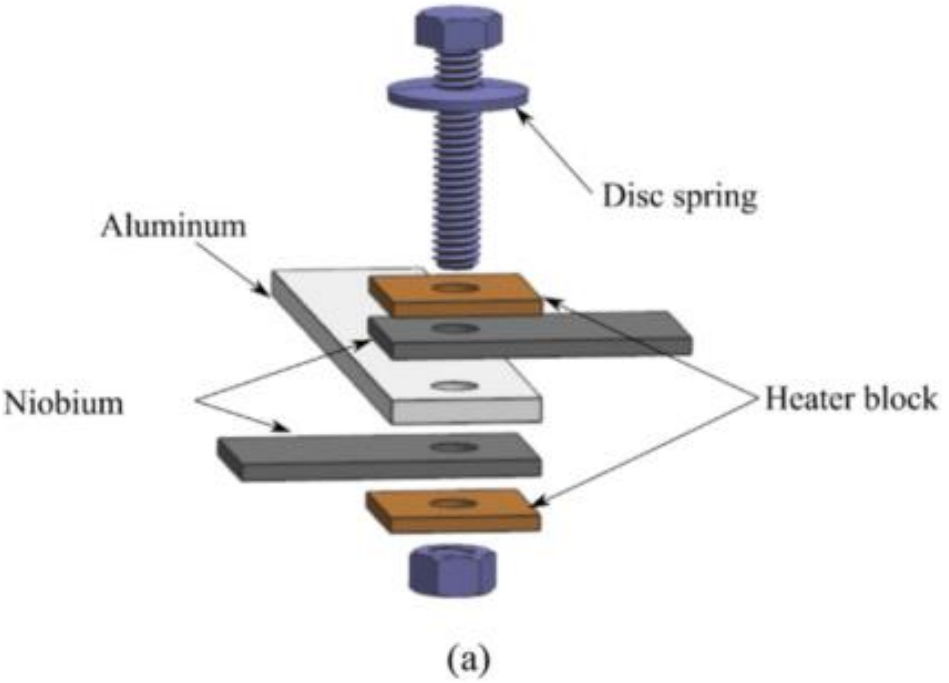

(a)

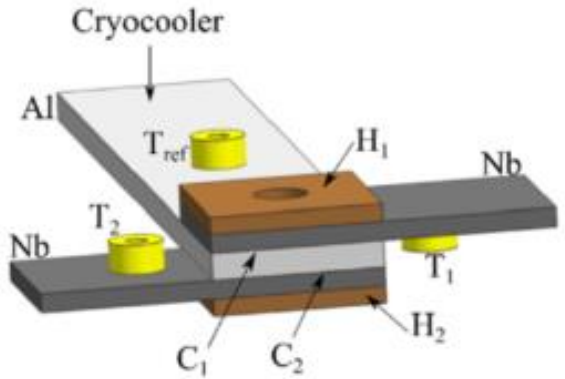

Dhuley et al. : https://doi.org/10.1016/j.cryogenics.2018.06.003

Fermilab

Nb-Al contact resistance: temperature dependence

Dry joints

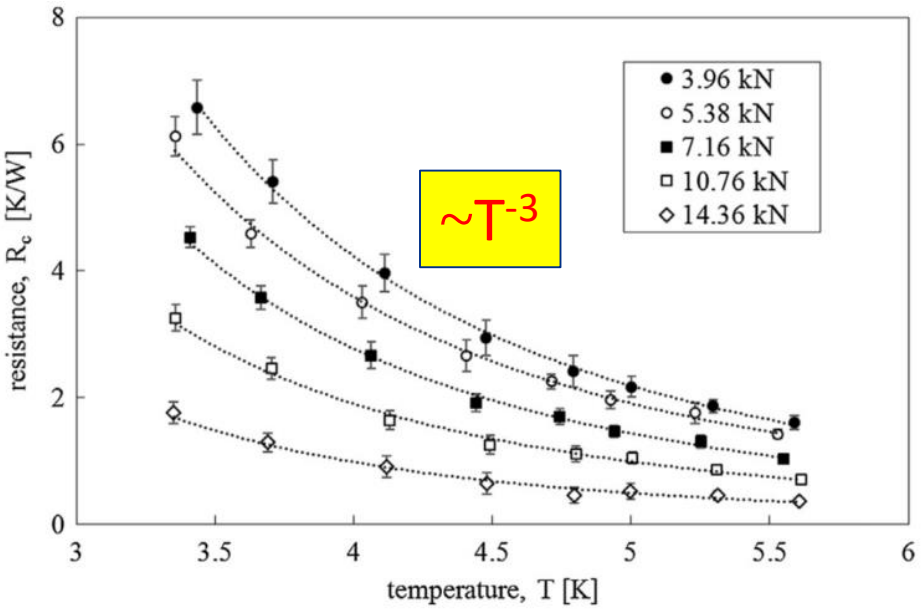

Joints with pressed indium foil

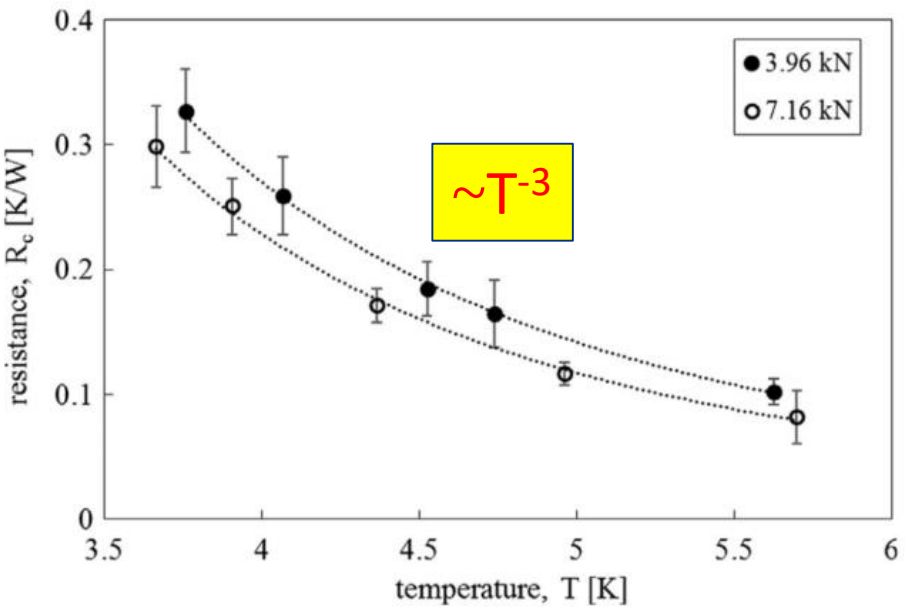

- Conduction electron density in Nb $n_e \sim \exp\left(\frac{-\Delta}{k_B T}\right)$
- Phonons increasingly dominate the heat transfer with decreasing temperature: $R_C \sim T^{-3}$

- 10x improvement with pressed thin foil indium (5 mils)
  - fills microscopic gaps
  - flow pressure ~2 MPa at room temperature, about four times higher near 4 K

Nb-Al contact resistance: force dependence

T = 3.5 K

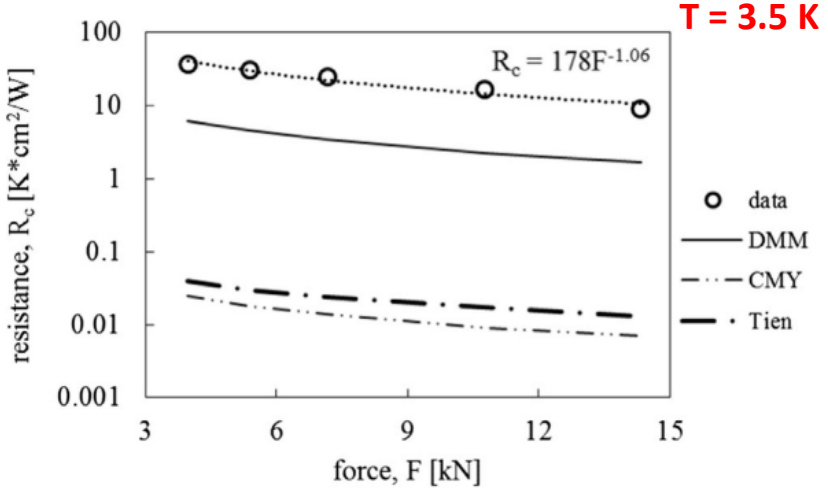

T = 4.0 K

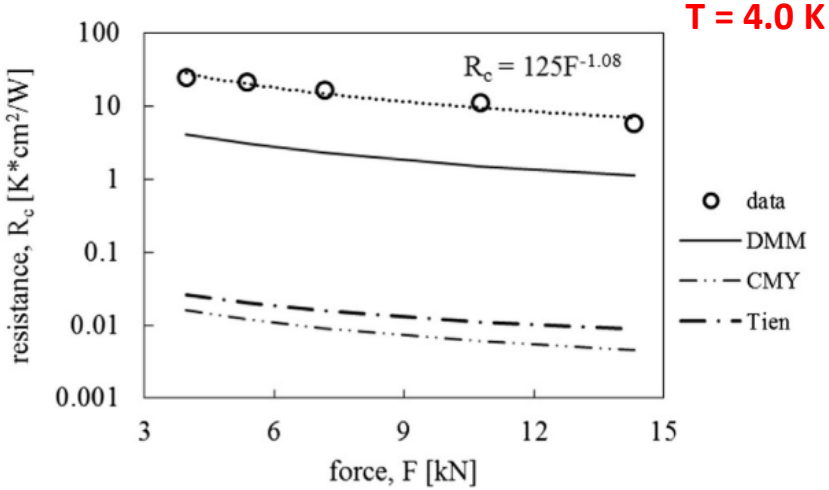

$$R_C \sim A_{real} \sim F^{-1}$$

T = 4.5 K

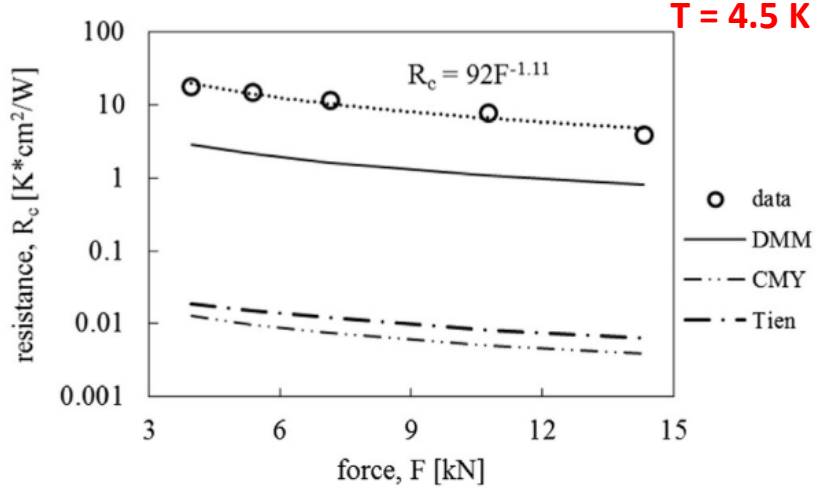

T = 5.0 K

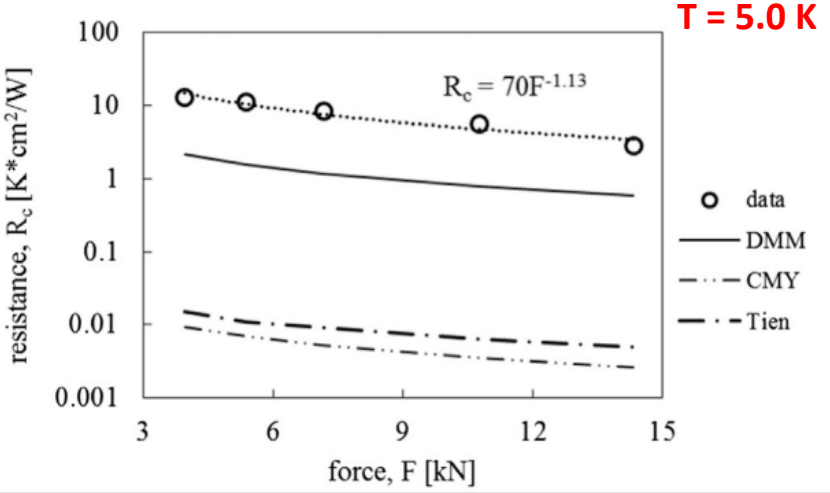

Reducing thermal resistance of pressed contacts

(Ref: Ekin)

	Type of pressure contact	Common method for lowering thermal resistance
1	Low pressure	Applying thermal grease (eg. Apiezon™ N) or varnish to each surface, thin layer of few microns
2	Moderate pressure (> yield strength of pure indium ~2 MPa)	Pressing 2 – 5 mils thick indium foil
3	High force	Gold plating surfaces, coating thickness > average surface roughness

- For joints with grease, varnish, or indium (p > 2 MPa) $A_{real} \approx A_{apparent}$, so contact resistance will scale with apparent surface area (joint size).
- For dry or gold-plated joints $A_{real} \ll A_{apparent}$, so the contact resistance will scale with force and not with apparent surface area.
- Resistance mitigation:
  - when large surface area is available, use grease with low pressure
  - when space is limited, use gold-plated surfaces with a large force

Reducing resistance across pressed contacts

Some methods of applying force

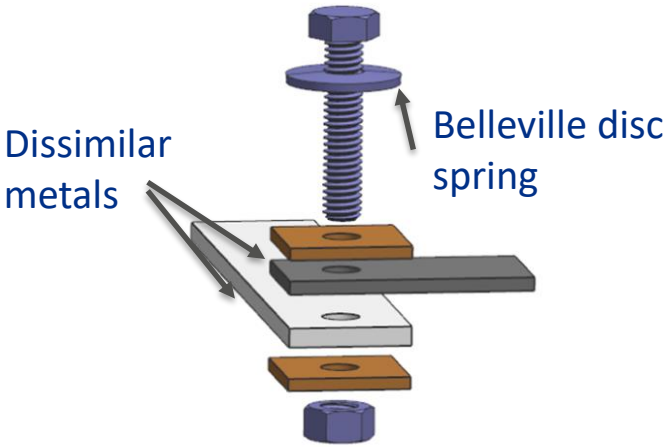

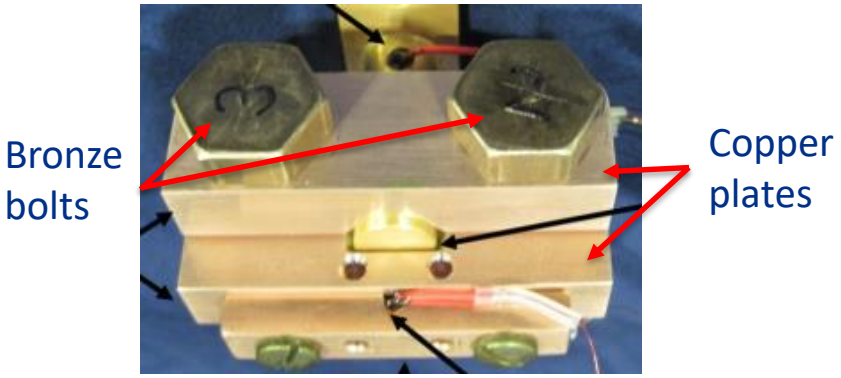

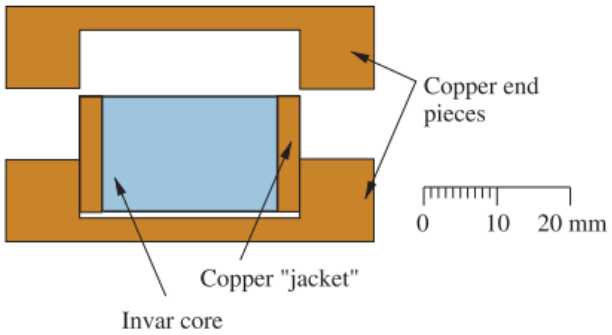

Bintley et al.: http://doi.org/10.1016/j.cryogenics.2007.04.004

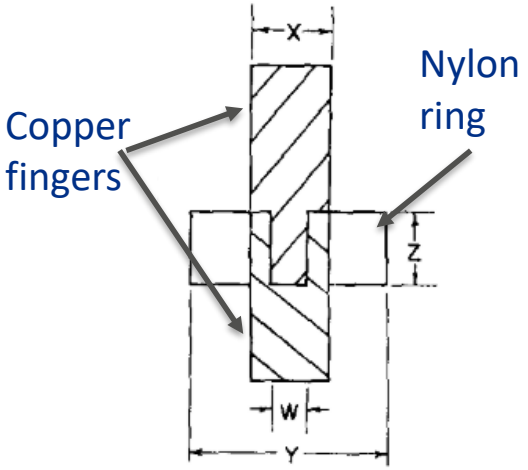

Boughton et al.: http://dx.doi.org/10.1063/1.1721058

Examples of data from literature

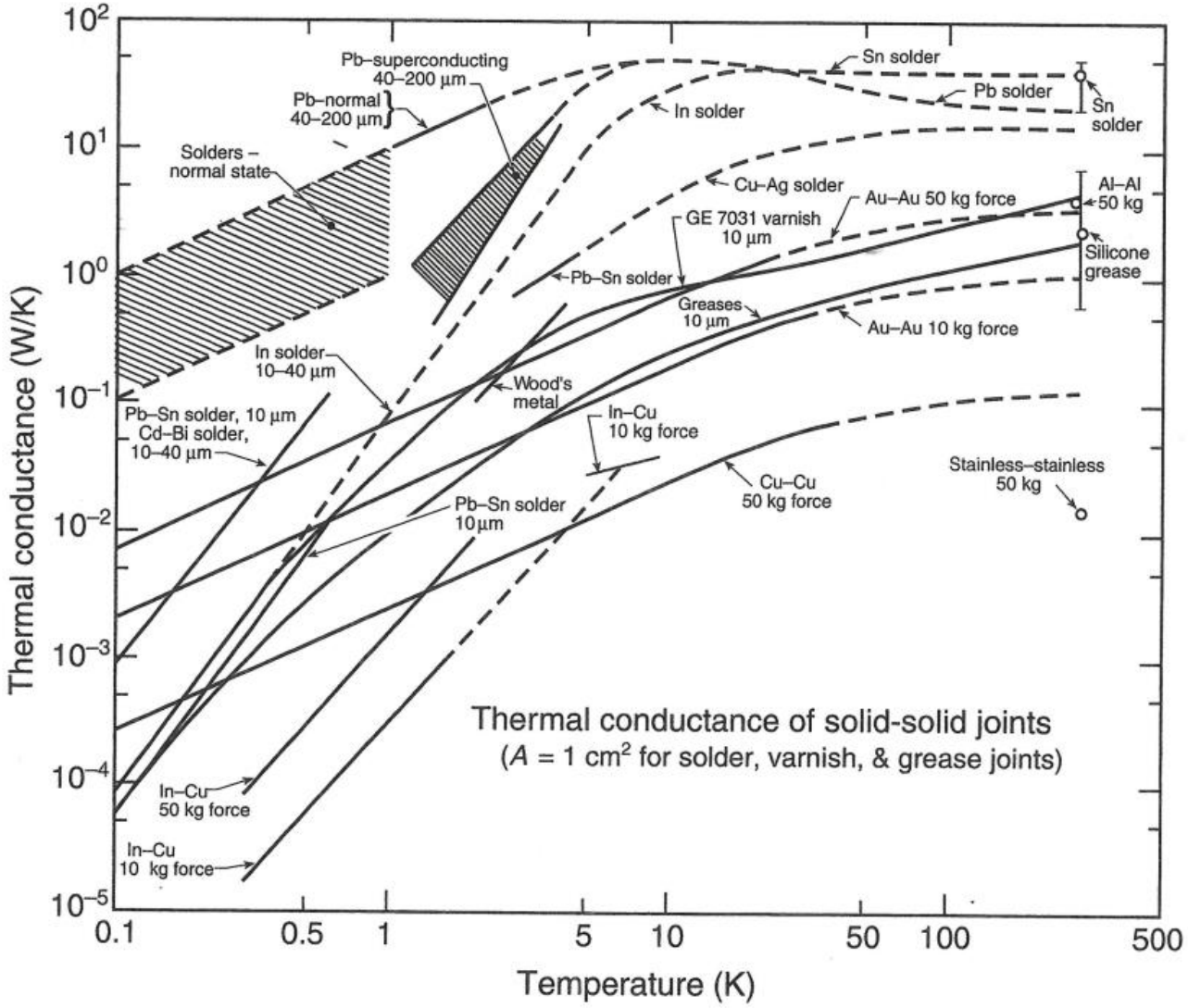

(From Ekin)

Fermilab

Examples of data from literature

Table II. Thermal Conductance of Metallic Contacts

	Material	Contact	Pressure (MPa)	h(W/cm^2 K)	Temp. Range (K)	Ref
1.	Al-Al (alloy)	machined	torque=20 Nm	$0.075\ T$	1.8-4.2	Wanner /13/
2.	Al-Al alloy	electropolished	torque=20 Nm	$3.6\times10^{-3}\ T^{2.3}$	1.8-4.2	
3.	Al-Al alloy	Au plated	torque-20 Nm	$1.9\times10^{-3}\ T^{1.4}$	1.8-4.2	
4.	Cu-Cu	machined	2.8	$4\times10^{-4}\ T^{2}$	1.8-4.2	Berman /8/
5.	Cu-Cu	machined	14	$1.67\times10^{-3}\ T^{2}$	1.8-4.2	
6.	Au-Au	--	5.6	$0.05\ T^{1.3}$	2-4	Berman & Mate /7/
7.	SS-SS (302)	polished	21	$0.014\ T^{1.5}$*	15-300	Lyon & Parrish /14/
8.	SS-SS (302)	polished	390	$0.10\ T^{1.5}$*	15-300	
9.	Cu-Cu	machined	7	$0.13\ T$	5-25	Nilles & Van Sciver /15/
10.	Cu-Cu	in solder	--	$7.5\ T$*	2-150	Radebaugh /16/
11.	Cu-Cu	Pb solder	--	$0.64\ T^{2.8}$	1.5-4	Challis & Cheeke /17/
12.	Cu-Cu	woods metal	--	$0.018\ T^{2.5}$	2-4	
13.	Cu-Cu	PbSn solder	--	$0.13\ T^{1.6}$	2.5-4	Foster /18/
14.	Al-Al	SnPb foil	26	$0.02\ T^{0.8}$*	10-300	Friedman & Gasser /19/
15.	Cu-Al	SnPb foil	9	$0.04\ T$*	10-300	
16.	Cu-Cu	SnPb Foil	7	$0.17\ T$*	10-300	

(From Van Sciver, Nilles, and Pfotenhauer)

Examples of data from literature

Table III. Electrical Boundary Resistance at Low Temperatures (T = 4.2 K)

Materials	Contact	P (MPa)	$\rho_B(\Omega\ cm^2)$	Ref.
Cu-Cu	cleaned	6.9	9.5×10^{-7}	Zar /20/
		20.7	6.3×10^{-7}	
Cu-Cu	Au plate	6.9	1.4×10^{-7}	
	Ag plate	6.9	1×10^{-8}	
Cu-Cu	Oxidized	340	1.4×10^{-8}	Noterdaeme et al. /5/
	Ag plate	170	1.5×10^{-9}	
	clean	170	5.6×10^{-9}	
Cu-Cu	cold weld	--	8×10^{-10}	Cornish et al. /21/
Cu-Cu	in foil	4 Nm torque	5×10^{-9}	Deutsch /22/
Cu-Cu	clean	4 Nm torque	5.7×10^{-8}	
Cu-Cu	clean	7	2.3×10^{-7}	Nilles & Van Sciver /15/
	thin oxide	7	5×10^{-7}	
	thick oxide	7	9×10^{-7}	
Al-Al	PbSn	--	$1.4\ 10^{7}$	Hartwig & Van Sciver /23/

(From Van Sciver, Nilles, and Pfotenhauer)

Examples of data from literature

Table I. Thermal Conductance of Insulating Contacts

	Material	Contact	Pressure (MPA)	h(W/cm^2 K)	Temp range (K)	Ref.
1.	In-sapphire	bonded	--	$0.03\ T^3$	1.4-2.1	Neeper & Dillinger /6/
2.	sapphire-sapphire	dry	4	$9 \times 10^{-6}\ T^3$	2-20	Berman & Mate /7/
3.	Cu-diamond	dry	4	$2 \times 10^{-5}\ T^3$	1.5-20	
4.	Cu-Teflon-Cu	12 mil foil	4	$1.8 \times 10^{-4}\ T^2$	2-5	Berman /8/
5.	Cu-epoxy-Cu	bonded	--	$0.09\ T^3$	0.05-0.25	Peterson & Anderson /2/
6.	Al-epoxy-Al	bonded	--	$0.13\ T^3$	0.05-0.25	
7.	Pb-epoxy-Pb	bonded	--	$0.40\ T^3$	0.05-0.25	
8.	Be-epoxy-Be	bonded	--	$0.013\ T^3$	0.05-0.25	
9.	Cu-LiF	Ge-7031	--	$0.05\ T^3$	0.4-1.3	Ackerman & Anderson /9/
10.	Cu-sapphire-Cu	dry	0.1	$1 \times 10^{-6}\ T^3$	1.5-4	Yoo & Anderson /10/
11.	Cu-sapphire-Cu	Al_2O_3	0.1	$2 \times 10^{-9}\ T^3$	0.8-3	
12.	Cu-epoxy-Cu	bonded	--	$0.16\ T^{0.5}$	2-8	Matsumoto et al./11/
13.	Cu-epoxy-Cu	bonded	--	$0.089\ T^{1.9}$	1-4	Schmidt /12/

(From Van Sciver, Nilles, and Pfotenhauer)

Examples of data from literature

TABLE I. Electrical resistances at 4.2 K for the joints of various combinations of metals including other works. For reference, the resistances at room temperatures, the resistance ratios, contact area, diameters of screws, and applied torques for fastening are listed only for this work.

Metal	Method of contact	Resistance at 4.2 K ($\mu\Omega$)	Resistance at 300 K ($\mu\Omega$)	Resistance ratio	Contact area (mm^2)	Diameter of screw (mm)	Torque (N m)
Platinum and silver	stainless-steel screw[a]	0.005	0.87	174	126	5	12
	brass screw[a]	0.011	0.91	79	126	5	6
	stainless-steel screw[a]	0.26	2.4	9.2	78	3	4
	brass screws[a]	0.097	2.8	29	78	3	2
	brass screws (platinum in fork-shaped silver)[a]	0.25	8.0	32	100	3	1
Platinum and copper	TIG weld[a]	17.5	310	18	10		
	spot weld[a]	3.2	358	112	9		
Silver and silver	EB weld[a]	0.018	0.91	50	16		
	silver screw[b]	0.1					
	brass and stainless-steel screws[c]	0.03					
Copper and copper	silver solder[d]	17					
	silver solder[e]	0.17					
	gold plated and nylon squeeze[e]	0.3					
	indium solder[f]	2.45					
	epoxy plate and screw[f]	1					
	tapered screw[d]	1.3					
	gold plated and screw[d]	0.4					
	tapered screw[f]	0.1					
	screw[f]	0.1					
	screw[g]	0.2					
	sanded and screws of brass and stainless steel[c]	0.13					
	chemically polished and screws of brass and stainless steel[c]	0.06					
	nylon squeeze[d]	0.04					
	gold plated and screws of brass and stainless steel[c]	0.04					
	TIG weld untreated[d]	0.034					
	TIG weld annealed[d]	0.013					

(From Mamiya et al.)

Examples of data from literature

Table 1. Summary of Thermal Contact Literature

Researcher (Reference)	Year	Material	Temp (K)	Applied Force (N)	Conductance (W/K)
Berman (1)	1956	Copper	4.2	223	5.5×10^{-3}
		"	"	446	1.02×10^{-2}
		"	"	670	1.46×10^{-2}
		"	"	892	1.9×10^{-2}
		"	"	1115	2.3×10^{-2}
Deutsch (12)	1979	Copper	4.2	1004	0.34
Kittel et al	1992	Au-plated:	1.6-4.2	22-670	1.3×10^{-4}
(8, 15)		Aluminum			to
		Brass			3.3×10^{-2}
		Copper			
		Stainless steel			
		Bimetallic:			9×10^{-3}
	1994	Alum & Stainless Steel	77	9-267	to 2.1×10^{-2}
Manninen & Zimmerman (13)	1977	Copper	4.2	1004	0.34
Mian et al (15)	1979	Mild steel	300	981	*0.825 †1.25

*optically flat

†roughness < 3μm

(From Salerno and Kittel)

Examples of data from literature

Table 1. Summary of Thermal Contact Literature (continued)

Researcher (Reference)	Year	Material	Temp (K)	Applied Force (N)	Conductance (W/K)
Nilles and Van Sciver (11)	1988	Copper	4-290	129	4×10^{-3}
		-oxidation treatment			1.4×10^{-2}
					2.0×10^{-2}
		-normal			8.0×10^{-2}
					1.3×10^{-1}
					1.4×10^{-1}
Radebaugh et al (17)	1977	Copper	4.2	490	10^{-2}
		Polished Ag	4.2	490	1.1
		Stainless Stl	300	490	10^{-2}
Salerno et al	1984	Aluminum	1.6-4.2	22-670	1×10^{-4}
(4, 5, 6, 7)	1985	Brass			to
	1986	Copper			2.0×10^{-2}
		Stainless Stl			
Salerno et al	1993	Augmented:	1.6-4.2	22-670	3.6×10^{-5}
(9, 10)		Aluminum			to
		Brass			1.0×10^{-2} (Au-plated Washer)
		Copper			
		Stainless Steel			5.0×10^{-4}
	1994				to
					0.28 (In, Ap)
Suomi et al (18)	1968	Copper	0.02-0.2	?	10^{-2}
Thomas & Probert (19)	1970	Stainless Steel	88-95	446	0.36
				892	0.5
Wanner (20)	1981	Aluminum	1-4	4683	**0.2
				9366	**0.6
				12488	**1.5
					**at 4.2 K

(From Salerno and Kittel)

Useful references

Overview of constriction resistance models

- Madhusudhana: https://www.springer.com/us/book/9783319012759
- Lambert and Fletcher: https://dx.doi.org/10.2514/2.6221
- Bahrami et al.: http://dx.doi.org/10.1115/1.2110231

Overview of boundary resistance models

- Little: https://doi.org/10.1139/p59-037
- Swartz and Pohl: https://doi.org/10.1103/RevModPhys.61.605
- Gundrum *et al.*: https://doi.org/10.1103/PhysRevB.72.245426
- Prasher and Phelan: https://doi.org/10.1063/1.2353704

Data at cryogenic temperatures (reviews)

- Salerno and Kittel: NASA NTRS 19970026086
- Mamiya *et al.*: https://doi.org/10.1063/1.1139684
- Van Sciver, Nilles, Pfotenhauer: Proc. SCW 1984
- Gmelin et al.: https://doi.org/10.1088/0022-3727/32/6/004
- Ekin: http://dx.doi.org/10.1093/acprof:oso/9780198570547.001.0001
- Dhuley:

"You are working on a very complex problem from both a mechanical and a thermal perspective. There are no simple solutions or models."

Michael M. Yovanovich

This document has been authored by Fermi Research Alliance, LLC under Contract No. DE-AC02-07CH11359 with the U.S. Department of Energy, Office of Science, Office of High Energy Physics.